Asian Review of Mechanical Engineering
ISSN: 2249-6289 (Print) | 3049-1886 (Online)
Journal Homepage: https://armejournal.org/
DOI: https://doi.org/10.70112/arme-2026.15.1.4323

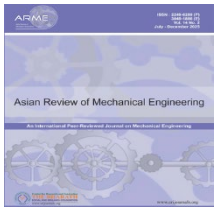

Research Article

Thermo Hydrodynamic Performance Analysis of Laminar Flow in Partially Porous Filled Channels: A CFD Study

Muhammad Haris Malik[1*], Zaryab Basharat[2], Fazal E Wadood[3], Muhammad Faizan Kahloon[4] and Daim Rabbani Awan[5]

[1*,4]Department of Fluid Machinery and Engineering, [2]MOE Key Laboratory of Thermo-Fluid Science and Engineering, Xi'an Jiaotong University, Xi'an, China,
[3]School of Engineering and the Environment, Kingston University, London, United Kingdom
[5]Department of Mechanical Engineering UET Lahore, Narowal Campus, Pakistan

Article Information

Article History
Received: 18 February 2026
Revised: 5 March 2026
Accepted: 27 March 2026
Published online: 5 April 2026

Keywords
Heat Transfer Enhancement
Porous Medium
Reynolds Number
Nusselt Number
Pressure Drop

Correspondence
muhammadharismalik3@gmail.com

ORCID
Muhammad Haris Malik
https://orcid.org/0009-0008-1618-4699
Zaryab Basharat
https://orcid.org/0009-0008-1914-3331
Fazal E. Wadood
https://orcid.org/0000-0003-4752-4357
Muhammad Faizan Kahloon
https://orcid.org/0009-0009-4011-6669
Daim Rabbani Awan
https://orcid.org/0009-0004-2193-0044

Abstract

This research presents a numerical study of laminar flow characteristics and thermal enhancement in a channel partially occupied by a porous medium. Computational simulations were carried out using ANSYS Fluent to examine the influence of particle diameter and viscous resistance on key thermal performance indicators, including the Nusselt number, pressure drop, and overall performance index, within a two-dimensional configuration. The porous structure was intentionally incorporated into the channel to improve heat transfer behavior. The permeability of the porous medium was determined using the Kozeny–Carman equation, and simulations were conducted for various Reynolds numbers and particle sizes. The results indicate that increasing particle diameter enhances heat transfer performance, whereas higher viscous resistance significantly increases pressure losses in the channel. At constant porosity, the Reynolds number exhibits minimal impact on the overall performance index. The findings confirm that porous materials can effectively augment heat transfer efficiency; however, excessive viscous resistance may adversely affect overall system performance.

I. INTRODUCTION

Heat transfer enhancement plays a vital role in many engineering systems, including thermal management technologies, energy conversion processes, electronic cooling applications, and industrial heat exchangers. Improving heat transfer efficiency while maintaining acceptable pressure loss remains a major challenge in thermal engineering design. Over the past few years, porous materials have gained considerable interest as a promising technique for heat transfer enhancement because of their high specific surface area, intricate flow structures, and ability to promote fluid mixing. The incorporation of porous structures within flow channels increases fluid–solid interactions, thereby enhancing the overall heat transfer capability of the system. Because of these advantages, porous media are widely

applied in various engineering fields such as heat exchangers, catalytic reactors, thermal insulation systems, and energy storage technologies. Previous investigations have shown that introducing porous materials into flow passages can significantly improve heat transfer rates by increasing effective thermal conductivity and disturbing the thermal boundary layer. However, the presence of porous media also introduces additional flow resistance, which results in higher pressure drop and increased energy consumption. A substantial body of experimental and numerical research has been devoted to examining fluid flow and heat transfer behavior within porous media. These investigations typically emphasize critical parameters such as porosity, permeability, particle size, and Reynolds number, as these factors significantly affect both hydrodynamic characteristics and thermal efficiency. CFD has become a key analytical tool for examining transport mechanisms in porous structures and predicting their performance under different operating scenarios. Flow through porous materials is generally modeled using the Darcy or Darcy–Forchheimer formulations, whereas permeability is commonly estimated using the Kozeny–Carman correlation. Despite the extensive research in this area, limited studies have examined the combined influence of particle diameter and viscous resistance on heat transfer and flow behavior under laminar flow conditions. In particular, the effects of porous medium properties on important performance indicators such as the Nusselt number, pressure drop, and overall thermal performance require further investigation to optimize system efficiency.

Accordingly, this study seeks to examine the heat transfer performance and laminar flow behavior in a channel partially occupied by a porous medium using numerical modeling techniques. The effects of particle diameter and viscous resistance on thermal performance, pressure loss, and performance number are analyzed using ANSYS Fluent. The permeability of the porous medium is estimated using the Kozeny–Carman equation, and the influence of the Reynolds number on system performance is also examined. The results of this study provide useful insights for improving heat transfer efficiency and optimizing porous medium design in thermal systems. In the momentum equation, the pressure drop is related to the bulk velocity.

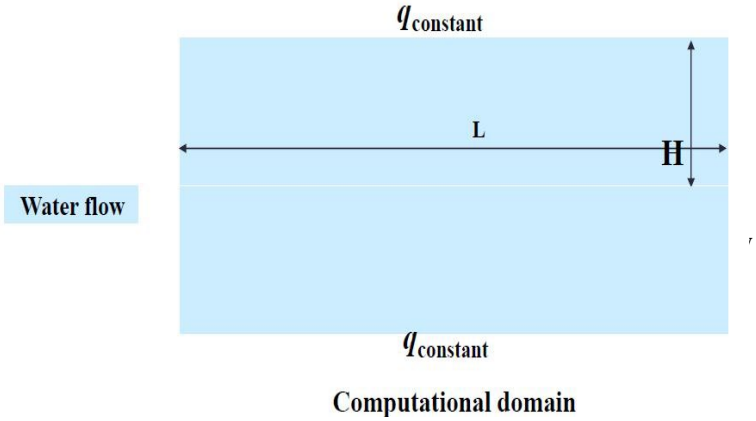

Fig.1 Schematic Representation of the Physical Domain

II. COMPUTATIONAL PROCEDURE

A. Mathematical Framework and CFD Implementation

The characteristics of fully developed laminar flow and the corresponding heat transfer were analyzed in a straight channel with a width of 0.4 cm and a length of 2 cm. A schematic representation of the physical domain considered in this investigation is presented in Figure 1. The shaded region denotes the porous medium, while the interconnected void spaces and channels are filled with liquid water. The total calculated area is 0.8 cm², and the porous dielectric layer is 0.2 cm thick. Porous media with different particle diameters and the same porosity are filled into the outer region, and the heat transfer and resistance characteristics of the multiple void regions with different properties are analyzed. The assumptions for the calculation are as follows:

1. The porous medium is uniform and isotropic.
2. The porous skeleton and fluid satisfy local thermal equilibrium.
3. At the entrance of the channel, the flow has already reached fully developed laminar conditions before entering the porous medium.
4. The calculation domain is a two-dimensional axisymmetric problem.

The numerical grid for the calculations was generated using ANSYS FLUENT [3], as shown in Figure 2. A structured grid was employed for the computational domain.A symmetry condition was applied along the centerline of the model, and the boundary conditions are presented in Table I.

TABLE I SUMMARY OF BOUNDARY CONDITIONS

Boundary	Condition
x = 0 (Inlet)	$v_x = U_{in}$, T = 300, K
x = L (Outlet)	p = 0, Pa, ($T_{backflow}$ = 300, K
y = H (Upper Wall)	$v_x = v_y = 0$, q = 500 W/m^2
Porous Region	Thermal-equilibrium model

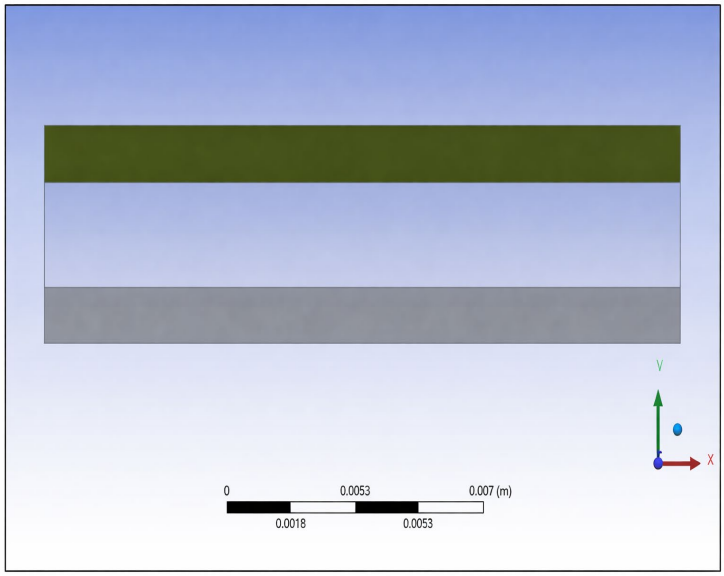

Fig.2 Structured Computational Mesh

In non-porous areas, the mathematical model of two-dimensional flow and heat transfer is

$$\frac{\partial \rho}{\partial t} + \nabla \cdot (\rho \mathbf{u}) = 0 \quad (1)$$

$$\frac{\partial (\rho \mathbf{u})}{\partial t} + (\mathbf{u} \cdot \nabla)(\rho \mathbf{u}) = -\nabla p + \eta \nabla^2 \mathbf{u} \quad (2)$$

$$\frac{\partial (\rho C_p T)}{\partial t} + (\boldsymbol{u} \cdot \nabla)\left(\rho C_p T\right) = \lambda \nabla^2 T + S \quad (3)$$

In the formula: U is x, y two direction speed; ρ is the density of water; P is fluid pressure; T is the thermodynamic temperature of fluid; Cp and λ are fluid fixed pressure ratio heat capacity and thermal conductivity. In porous areas, the continuous equations of two-dimensional flow and heat transfer are:

$$\frac{\partial (\varepsilon \rho)}{\partial t} + \nabla \cdot \left(\varepsilon \rho \mathbf{u}_{physical}\right) = 0 \quad (4)$$

The momentum equation is:

$$\frac{\partial (\rho \mathbf{u})}{\partial t} + (\mathbf{u} \cdot \nabla)(\rho \mathbf{u}) = -\nabla p + \eta \nabla^2 \mathbf{u} \quad (5)$$

The energy equation is:

$$\frac{\partial ((\rho C_p)_{eff} T)}{\partial t} + \left(\mathbf{u}_{superficial} \cdot \nabla\right)\left(\rho C_p T\right) = \lambda_{eff} \nabla^2 T + S_{eff} \quad (6)$$

For non-compressible steady-state problems:

$$\nabla \cdot \mathbf{u}_{superficial} = 0 \quad (7)$$

$$\left(\frac{\mathbf{u}_{superficial}}{\varepsilon} \cdot \nabla\right)\left(\mathbf{u}_{superficial}\right) = -\frac{1}{\rho} \varepsilon \nabla (p) + \eta \nabla^2 \left(\mathbf{u}_{superficial}\right) + \mathrm{F} \quad (8)$$

$$\mathrm{F} = -\frac{\varepsilon \upsilon}{k} \mathbf{u}_{superficial} - \frac{\varepsilon F_\varepsilon}{\sqrt{k}} |\mathbf{u}_{superficial}| \mathbf{u}_{superficial} \quad (9)$$

In the formula, ε represents the porosity of the porous medium; K represents the permeability of the porous medium; F denotes the momentum source; and the subscript "superficial" refers to the apparent value. In Equation (8), the first term represents the viscous component, and the second term represents the inertial component.

In FLUENT, the formula (8) is expressed in the following formula:

$$\mathrm{F} = -\frac{\mu}{k} \mathbf{u} - C_2 \frac{1}{2} \rho |\mathbf{u}| \mathbf{u} \quad (10)$$

Formula: K for permeability; C_2 for inertial resistance; viscous resistance for 1/k, if the fluid flow rate is very small, the second item can be omitted. For the porous dielectric region composed of two groups of solid particles with different diameters, the k is calculated by using the Ergun equation and equation (10).

$$\frac{\Delta P}{l} = \frac{150 \mu}{D_P^2} \frac{(1-\varepsilon)^2}{\varepsilon^3} u + \frac{1.75 \rho}{D_P} \frac{(1-\varepsilon)}{\varepsilon^3} u^2 \quad (11)$$

The equation (10,11) draws

$$\mathrm{k} = \frac{D_P^2}{150} \frac{\varepsilon^3}{(1-\varepsilon)^2} \quad (12)$$

$$C_2 = \frac{3.5}{D_P} \frac{(1-\varepsilon)}{\varepsilon^3} \quad (13)$$

TABLE II PARTICLE DIAMETER AND ITS CORRESPONDING VISCOUS RESISTANCE

The diameter of solid particle	Viscous resistance
100×10^{-6}	3.33×10^{-11}
50×10^{-6}	4.1×10^{-11}

TABLE III RE NUMBER AND ITS CORRESPONDING ENTRY SPEED

Re	U
10	4.9×10^{-3}
20	9.98×10^{-3}
30	1.49×10^{-2}
40	1.94×10^{-2}

B. Solution Methods and Convergence Criteria

Numerical computations were performed using ANSYS Fluent to simulate the flow and heat transfer behavior. The governing equations for velocity, pressure, and temperature were solved using the SIMPLE pressure–velocity coupling scheme in the microchannel domain [4]. An unstructured mesh consisting of rectangular elements was generated for the SOHC microchannels, with mesh refinement applied near the offset rib regions to accurately capture flow variations. A non-uniform grid distribution was adopted, with a higher mesh density in critical regions. Solution convergence was achieved when the normalized residuals fell below 10^{-6} for the energy equation and 10^{-3} for all other governing equations. The numerical model was validated to ensure solution accuracy. A grid independence analysis was conducted for the microchannel heat sink by testing different mesh densities. The final computational grid selected for the simulations consisted of approximately 0.2013 million elements.

C. Formation of Geometry

Simulations at the pore level are very difficult to perform. Firstly, the required geometry is difficult to create. The entire analysis is based on a two-dimensional model; therefore, for the purpose of geometry sketching, the 2D analysis type was selected. While sketching on the XY-plane, a rectangle was created for the geometry, and the dimensions were applied according to the specified thickness. Three separate sketches were drawn: one for the water zone and the other two for the porous zones. After that, the geometry was completed using the “Add Frozen” option.

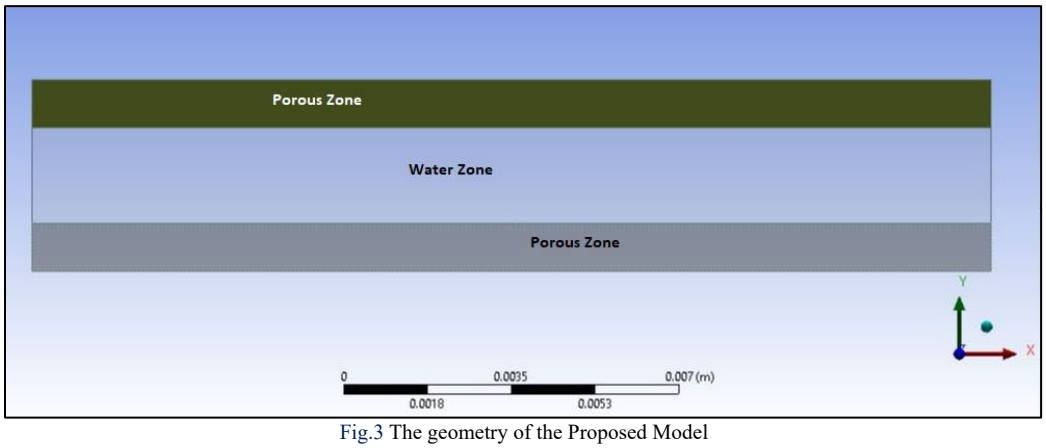

Fig.3 The geometry of the Proposed Model

D. Mesh Generation

The computational model was implemented using ANSYS Fluent for numerical analysis. Laminar flow conditions were assumed throughout the simulation, and thermal radiation effects were excluded. The density of air in the annular region was modeled using the Boussinesq approximation [5], while no-slip conditions were imposed on the solid boundaries. A high-resolution mesh was employed to enhance solution accuracy. Several steps were followed in generating the mesh. For sizing, all edges of the water and porous zones were selected. The mesh behavior was set to hard. During the mesh refinement process, the element size was specified, and the model was then updated.

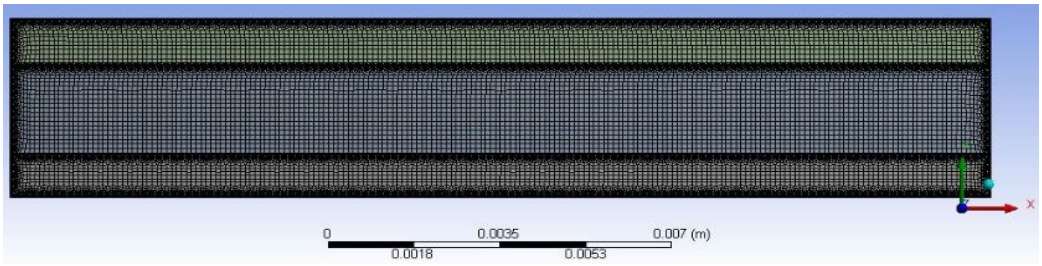

Fig.4 Mesh generation

E. Computational Domain and Boundry Conditions

The computational domain, coordinate system, and relevant notations are illustrated in Figure 1. The fluid viscosity at the porous medium inlet is assumed to be temperature-dependent and is determined based on Reynolds numbers ranging from 0 to 50.

At the inlet boundary ($x = 0$), a uniform velocity and temperature are prescribed as:

$$V = U_{in}, T = 300\ K$$

where $U_{in}$and Trepresent the inlet fluid velocity and temperature, respectively. At the outlet boundary ($x = L$), a pressure-outlet condition is imposed.

X = L: p = 0 Pout Pa

Where Pout is the specified pressure. For the inner wall fluid contact surface.

u = v = w = 0,

$$-k_s\ \partial Ts/\partial n = -k_f\ \partial Tf/\partial n$$

Where n is the local coordinate normal to the wall.

F. Setup Generation

For the setup generation, it is necessary to enable all relevant equations, such as the energy equation and laminar flow. The material selected from the Fluent database should be liquid water. The following values were entered in the setup domain:

Thermal Conductivity = 0.597 $W_m^{-1}K^{-1}$
Viscosity = 0.000998 Kg_m^{-3}
Porosity = 0.5
Velocity = 0.0049 ms^{-1}: 0.00998 ms^{-1}: 0.0149 ms^{-1}: 0.0194 ms^{-1}
Reynold no. 0 to 50
Thermal Heat Flux = 500 Weber
In the cell zone condition, put out the water liquid material and in a porous zone that is fluid putting the values of k.
$K_1 = 3.33 \times 10^{-11}$: $K_2 = 4.1 \times 10^{-11}$:

Now in the boundary conditions of inlet porous zone and water inlet zone, put out the values of velocity with all the values of k. Then initialize all the values.

III. HEAT TRANSFER AND FLOW CALCULATION

To analyze the heat transfer and resistance characteristics in the tube, the heat transfer coefficient hhh and the Nusselt number NuNuNu are defined by Equations (14) and (15) [6]:

$$h = \frac{Q}{\pi dL(T_w - T_f)} \quad (14)$$

$$Nu = \frac{hd}{\lambda} \quad (15)$$

In the above expression, Ddenotes the width of the channel, and Lrepresents its length. $T_w$corresponds to the wall temperature, while $T_f$indicates the fluid temperature. The parameter $k$refers to the thermal conductivity of the stationary fluid.

The comprehensive performance evaluation factor, which accounts for both heat transfer enhancement and flow resistance, is defined as follows:

$$PN = \frac{Nu/Nu_{base\ case}}{\Delta p/\Delta p_{base\ case}} (16)$$

To improve the PN value of enhanced heat transfer, metal materials are filled outside the circular tube as porous media.

IV. NUMERICAL DATA ACQUISITION

The parameters that define fluid flow and heat transfer processes in laminar flow are of interest in this study. The Reynolds number is given by the equation

$$R_e = \frac{\rho Uinlet\ H}{\mu}$$

The Reynolds number (Re) is a fundamental dimensionless parameter in fluid mechanics used to characterize flow regimes and predict the transition between laminar and turbulent behavior. At low Reynolds numbers, viscous forces dominate, resulting in smooth and orderly laminar flow. In contrast, higher Reynolds numbers indicate the increasing influence of inertial forces, leading to velocity fluctuations and directional instabilities within the fluid. These disturbances promote the formation of vortices and eddies, which enhance mixing but also increase energy dissipation. The intensified turbulence may contribute to pressure losses and can potentially increase the risk of cavitation under certain flow conditions [6].

The Reynolds number has a wide range of applications, from fluid flow in pipes to airflow over aircraft wings. It is used to predict the transition from laminar to turbulent flow and to compare similar flow conditions at different scales, such as between a model aircraft and a full-scale version in a wind tunnel [7].

V. RESULTS AND DISCUSSION

As the flow structure has a crucial effect on the heat transfer process, the assumptions of laminar flow and a porous medium were adopted. Using Fluent software, the energy and continuity equations were solved. The flow structure of the porous medium was analyzed, and the corresponding values were presented graphically.

The case file and data obtained from the Fluent software were processed, and the key parameters were extracted using the data-processing functions available in the software. The variation in Reynolds number is mainly reflected in the average inlet velocity. Based on the commonly used CFD commercial software ANSYS, the governing equations are solved using the Reynolds-averaged Navier–Stokes (N–S) equations, and a pressure-based segregated solver is selected. Because the Reynolds number does not exceed 400, turbulence effects are not considered. In addition, since the temperature is not high, radiative heat transfer is neglected. Therefore, the model is treated as laminar flow [8].

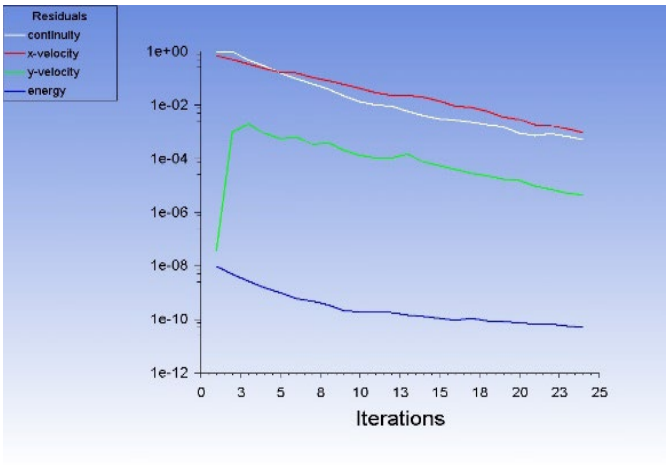

Fig.5 Residuals of Energy and Continuity Equations

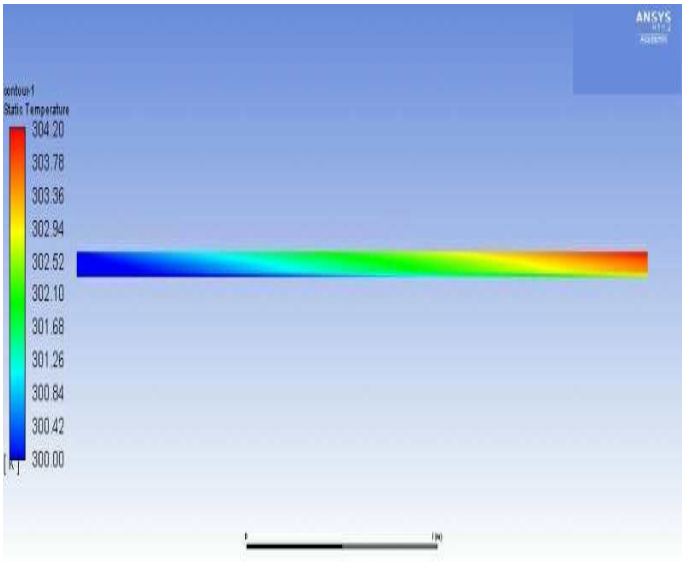

Fig.6 Temperature Contour Distribution

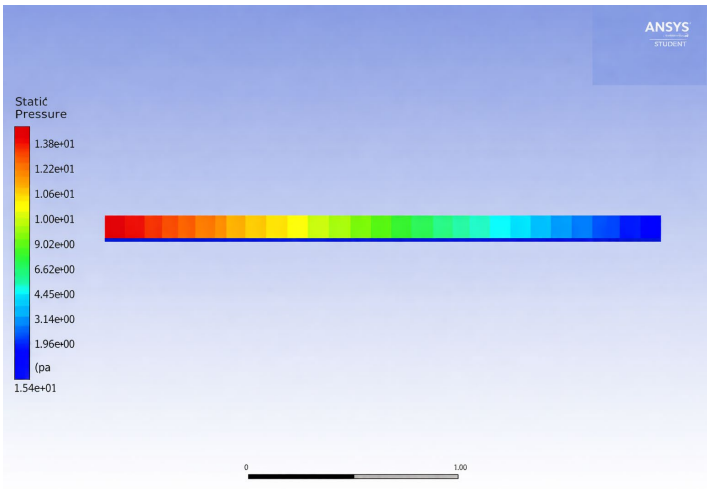

Fig.7 Pressure Contour Distribution

The above figure shows the variation in static temperature as the water flows through the channel from the inlet and illustrates the heat transfer phenomenon occurring as the water passes through the porous medium.

The above figure shows the variation in static pressure as the water flows through the channel from the inlet, and illustrates the pressure drop that occurs due to frictional effects as the water flows along the surface of the channel.

A. Comprehensive Performance Evaluation of Pressure drop, Nu and PN Numbers on Flow

Figure 8 shows a pressure drop diagram for two sets of particle diameters along the flow direction under different operating conditions. The magnitude of the pressure drop can indirectly indicate the strength of fluid flow resistance. It can be observed that, in the case of the same porosity (k = 0.5), the diameter of the metal particles constituting the porous medium has a significant impact on the pressure drop. The smaller the particle diameter, the greater the viscous resistance; consequently, the pressure drop increases significantly. The pressure drop mainly occurs in the inlet section, directly manifested by a large inlet pressure gradient, while the pressure drop in the mainstream region is relatively small due to boundary layer formation. At the same time, when the viscous resistance is relatively low, the Reynolds number has little effect on the pressure drop. However, under conditions of high viscous resistance, the Reynolds number has a significant effect on the internal pressure drop of the channel and cannot be ignored.

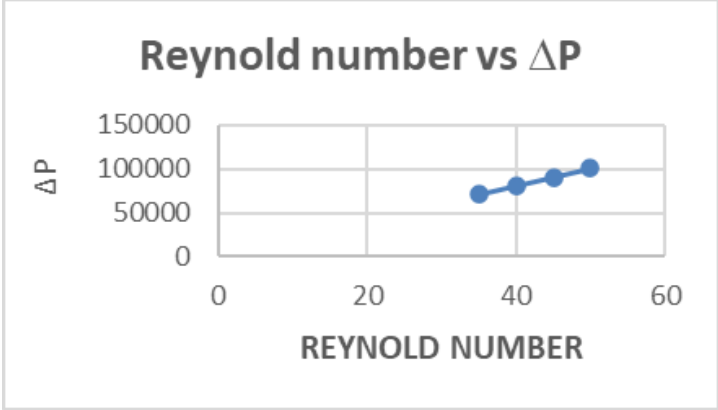

Fig.8 Variation of Pressure Drop (ΔP) with Reynolds Number

Figure 9 shows the Nusselt number of the inner wall corresponding to two different particle diameters. The overall trend of convective heat transfer variation on the surface with respect to the Reynolds number can be observed intuitively. The analysis indicates that the Nusselt numbers of porous media composed of two different particle diameters do not differ significantly under multiple operating conditions; however, the Nusselt number increases noticeably with increasing particle diameter. When the particle diameter is 0.00005, the Nusselt number remains below 50, and the increasing trend is gradual. Under the same porosity, a larger particle diameter reduces the overall viscous resistance, resulting in a longer boundary layer formation in the inlet section and an improved surface heat transfer coefficient. Consequently, the Nusselt number is enhanced to a certain extent.

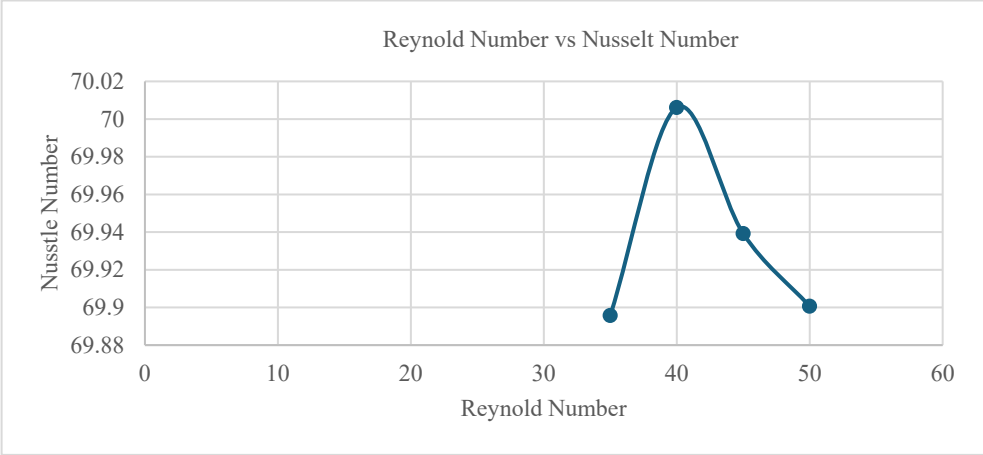

Fig. 9 Variation of Nusselt Number with Reynolds Number

Figure 10 shows the ratio of the Nusselt number to the pressure drop, referred to as the PN number, which reflects a comprehensive performance evaluation coefficient of convective heat transfer and flow resistance. The figure illustrates the variation of the PN number with respect to the Reynolds number (Re). As observed, for both particle diameter cases, the PN number exhibits a similar decreasing trend as Re increases. Although the pressure drop increases with higher Reynolds numbers due to enhanced viscous and inertial resistance, the PN number declines because the rate of heat transfer improvement does not proportionally compensate for the rise in flow resistance.

At low Reynolds numbers, the PN number decreases more rapidly, indicating greater sensitivity to flow variations in this regime. However, as Re continues to increase, the rate of change in the PN number gradually diminishes, and the curves tend to stabilize, approaching a relatively low and nearly constant value. To enhance heat transfer from the perspective of the PN number, a porous medium can be selected under certain operating conditions. The simulation results show that it can strengthen the overall heat transfer performance to a certain extent.

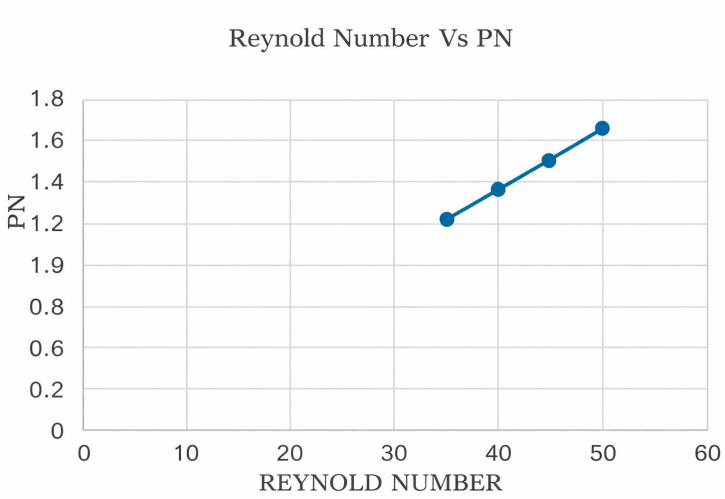

Fig. 10 Variation of Performance Number (PN) with Reynolds Number

VI. CONCLUSION

This study utilized Computational Fluid Dynamics (CFD) simulations performed in ANSYS Fluent to examine heat transfer enhancement and laminar flow characteristics in a channel partially occupied by a porous medium. The investigation was conducted by solving the discretized governing equations of momentum and energy to assess the effects of metal particle diameter and viscous resistance within the porous structure on thermal performance, pressure drop, and overall system efficiency. The numerical results demonstrate that the particle size of the porous medium significantly influences heat transfer enhancement in the fully developed laminar flow regime. Larger particle diameters contribute to improved thermal performance, whereas smaller particles provide comparatively limited enhancement. Moreover, the analysis indicates that viscous resistance has a pronounced impact on pressure loss across the channel. An increase in viscous resistance intensifies the pressure gradient, which may adversely affect the overall efficiency of the system.

Declaration of Conflicting Interests

The authors declare no potential conflicts of interest with respect to the research, authorship, and/or publication of this article.

Funding

The authors received no financial support for the research, authorship, and/or publication of this article.

Use of Artificial Intelligence (AI)-Assisted Technology for Manuscript Preparation

The authors confirm that no AI-assisted technologies were used in the preparation or writing of the manuscript, and no images were altered using AI.

REFERENCES

[1] K. Vafai, *Handbook of Porous Media*, 2nd ed. Boca Raton, FL, USA: CRC Press, 2005.
[2] D. A. Nield and A. Bejan, *Convection in Porous Media*, 4th ed. New York, NY, USA: Springer, 2013.
[3] S. V. Patankar, *Numerical Heat Transfer and Fluid Flow*. New York, NY, USA: Hemisphere Publishing, 1980.
[4] J. Bear, *Dynamics of Fluids in Porous Media*. New York, NY, USA: Dover Publications, 1988.
[5] ANSYS Inc., *ANSYS Fluent Theory Guide*, Release 2021 R1. Canonsburg, PA, USA: ANSYS Inc., 2021.
[6] F. P. Incropera, D. P. DeWitt, T. L. Bergman, and A. S. Lavine, *Fundamentals of Heat and Mass Transfer*, 7th ed. Hoboken, NJ, USA: Wiley, 2011.
[7] A. Bejan, *Convection Heat Transfer*, 4th ed. Hoboken, NJ, USA: Wiley, 2013.
[8] S. Whitaker, "Flow in porous media I: A theoretical derivation of Darcy's law," *Transport in Porous Media*, vol. 1, no. 1, pp. 3–25, 1986.
[9] P. Forchheimer, "Wasserbewegung durch Boden," *Zeitschrift des Vereins Deutscher Ingenieure*, vol. 45, pp. 1781–1788, 1901.
[10] M. Kaviany, *Principles of Heat Transfer in Porous Media*, 2nd ed. New York, NY, USA: Springer, 1995.